Influence of delamination on microtexture and J-R curve in API X60 steel

Ederson Pauletti[1], Hudison L. Haskel[1], Juliana P. Martins[2], André L M Carvalho[1*]

[1] Department of Materials Engineering, States University of Ponta Grossa-UEPG
[2] Department of Chemical Engineering, Federal Technological University of Paraná-UTFPR
* Corresponding author: andrelmc@uepg.br

Abstract: Large–diameter, high-pressure gas transmission pipelines have been used more and more widely all over the world. With the development of the pipeline network, safety and maintenance become an important task. Controlled thermo-mechanical processing is considered as the primary route for the development of API grade linepipe steels because it provides desirable and fine grained microstructure. It is known that crystallographic orientation can generate anisotropy of mechanical properties. Furthermore, studies on pipeline steels, such as X60, X70 and X80, suggest that delamination phenomenon the fracture surface in fracture toughness test specimens affects the measured fracture toughness and therefore safety evaluation of pipeline steels. Microtexture analysis by electron backscattering diffractions (EBSD) was carried out to obtain crystallographic orientation from the fracture process in which occurs the delamination phenomenon. Experimental results obtained by EBSD technique have shown that delamination phenomenon occurs in the {100}<011>crystallographic orientation. The α fiber texture such as :{113}<110>, {112}<110> and {223}<110>, have produced anisotropic mechanical properties that during fracture process act to reduce the plastic constraint and contributing to increase the stress plane

Keywords Delamination, fracture toughness test , crystallographic orientation, API X70 steel

1. Introduction

One of the most widely used classes of steel pipes is based on the standard API (American Petroleum Institute), which are classified according to chemical composition and mechanical properties [1]. These steels generally undergo thermomechanical processing, associated with addition of alloying elements such as Nb and Ti to obtain a material with high toughness and ductility, as well as good weldability, well known as HSLA steels (high strength low alloy) [2]. The thermomechanical processing imposed on HSLA leads to generation of preferential orientation (texture), resulting in anisotropy mechanical properties [3-6]. The occurrence of texture is most evident during the controlled rolling process which can produce recrystallization, transformation and deformation texture [3].

Special attention should be given the {100} <110> texture component which is parallel to the rolling plate direction. During the monotonic and dynamic test this component contributes to the occurrence of cleavage planes [3, 7 ,8 ,9, 10]. This cleavage planes also contribute to appearance of the delamination (split), as can be seen in Fig. 1. Other factors leading to the occurrence of delaminations are the formation of precipitates at grain boundaries [11, 12], inclusions [13, 14], elongated grains [11, 15], decohesion of grain boundaries [13, 14].

The aim of present work was to investigate the microtexture from the delamination region takes

place in the API 5L X70 steel during fracture process from the fracture toughness testing. Evaluation of microtexture and Taylor factor mapping were performed from the EBSD technique in the perpendicular region to the propagation fracture direction where delamination occurred.

2. Experimental Procedure

The material used in the investigation was obtained from an API X60 steel plate grade of 5/8 inch thickness. Table 1 shows the chemical composition of API X60 steel and the requirement of the API standard.

Table 1. Chemical Composition obtained for API X60 steel and maximum specification through API standard (in wt. %) [1].

Element	C	Mn	P	S	Ni +V+T	Cr	Cu	Co	Si
Composition	0,15	1,45	0,014	0,005	0,011	0,032	0,037	0,02	0,3
API Specification	0,26	1,40	0,030	0,030	0,015				

To obtain the tensile properties, three specimens from the rolling direction (RD) and transverse direction (TD) were extracted in each direction. The specimens were tested in tensile testing SHIMADZU machine at room temperature according to ASTM E8M [16].

The single edge tension SE(T) specimens were used to obtain *J-R* curves. All specimens crack planes were oriented in the LT orientation according to ASTM E1820 [17]. The SE(T) specimen has following dimensions: length of reduction section of 156 mm, radius of fillet of 10 mm, overall length of 276 mm, width, W, of 32 mm and thickness of 12.5 mm. This specimen was loaded with a centered pin at center distance of 214 mm. Crack length to width ratios of 0.21 and 0.52 were investigated, corresponding shallow and deep cracks respectively. The specimens were loaded in three-point bending with a span of 128 mm, after precracking by fatigue according to the procedure in ASTM E1820. The specimens were side grooved using a Charpy cutter to a total thickness reduction of 20%, in an attempt to develop plane strains conditions along crack front. The fracture toughness tests were performed in MTS Flex Test GT servo hydraulic machine according to ASTM E1820 [17]. All specimens were tested at room temperature. The J-R curves were obtained from unloading compliance technique using clip gage to measure the crack mouth opening displacement (CMOD). Procedure to calculate the J-R resistance such as, k, η, γ factors were obtained from the results of Cravero [18].

Microstructure analysis were performed from the rolling direction (RD), transverse (TD) and normal direction (ND) which were grinding, polished and chemically etched with Nital 2%.

The microtexture was carried out by EBSD technique. The sample was obtained from perpendicular fracture surface in the delamination region, as can be seen in Figs. 1.a e 1.b. Samples were polished in the solution of OP-S (colloidal silica), and then etched with Nital 2%. For EBSD data collection was used software TSL 5 IOM Data collection and for data processing was used software OIM Analysis 5. The scanning electron microscope used for performing of such measures was the EDAX TSL EVO MA 10.

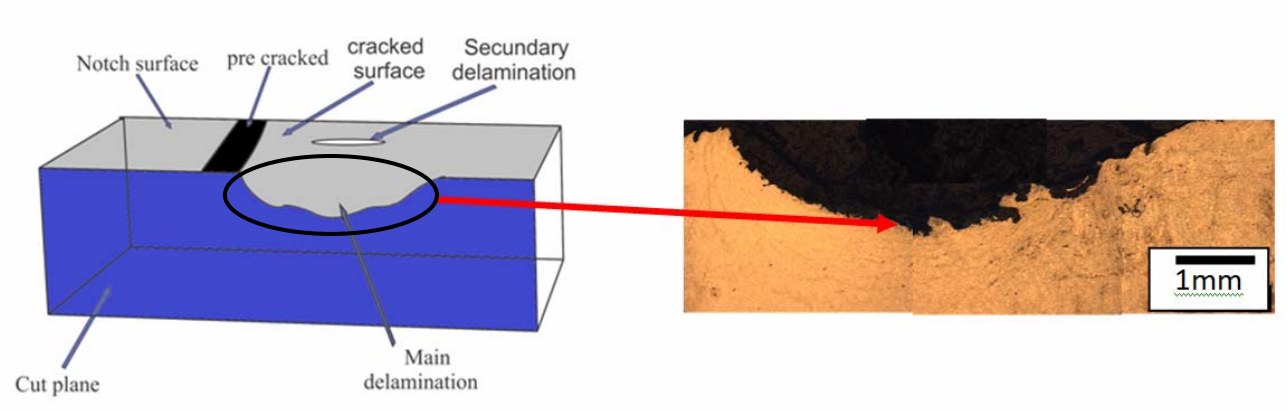

Figure 1 a) Schematic drawing shows the specimen section where was made cut perpendicular to the fracture surface b) fractured surface from the delamination region.

The scan was performed with step size of 1μm and magnification of 1000 times. Pole figures were obtained from the (100), (110) and (111) centered planes. While orientation distribution functions (ODF) was performed from the Euler space and the Bunge notation. Whereas, Taylor factor maps and misorientation angles distribution were generated in software for further analysis.

3. Results and Discussion

The chemical composition is according to the API standard [1], as shown the Table 1. The tensile properties obtained for the API X70 steel are shown in Table 2. The yield strength (YS), ultimate tensile strength (UTS) and elongation values are according to API standard [1].

Table 2. The tensile properties obtained from the tensile test for API X70 steel.

YS (MPa)	UTS (MPa)	Elongation (%)	Hardening exponent (%)	Modulus Elastic (GPa)
515	586	23	15	207

Fig. 2.a shows the three dimensional view of the API X70 microstructure steel. It can be observed a microstructure consisting of alternated layer of ferrite and pearlite in the RD and TD directions as also random distribution of ferrite and pearlite in the DN direction. Fig. 2.b shows the delamination region which can be noticed the banded microstructure caused by delamination.

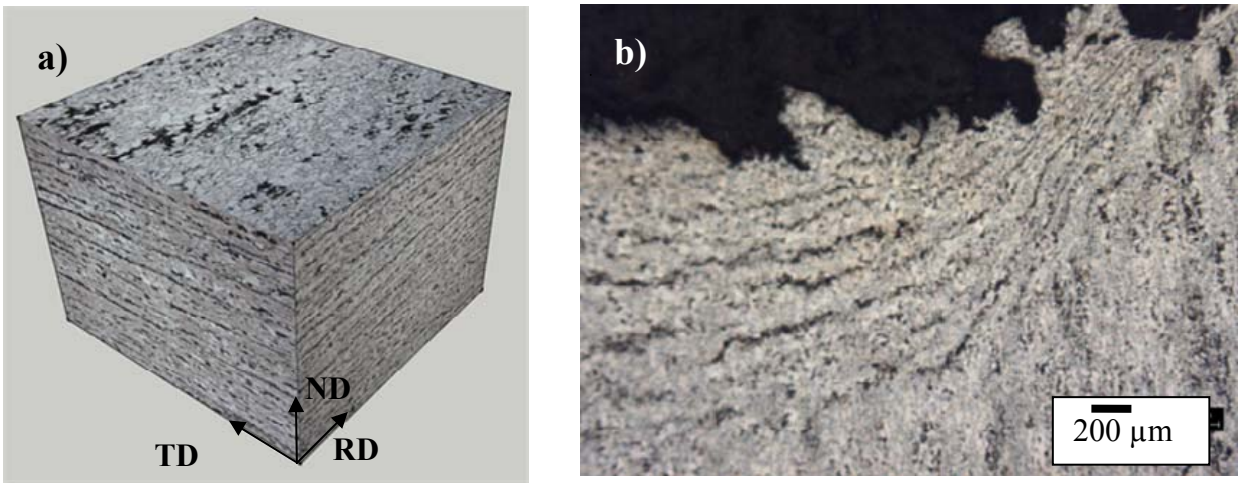

Figure 2. Microstructure of API X70 steel: a) three-dimensional view of the API X70 steel microstructure b) banded microstructure in the delamination region.

Fig. 3.a shows the fractured surface from tested specimen where it can be seen the notch, pre-fatigue crack, ductile crack extension. As the out-of-plane constraint is highest at the centre of the specimen, accordingly the delamination is most severe. Secondary delaminations are concentrated at the 1/4 thickness points from the free surfaces and similar to the main delamination [19, 20]. Fig. 3.b shows the P x CMOD curve from the unloading compliance method indicating the occurrence of delamination on the curve. It is possible to notice load-displacement curve a degree or register sequence failure. This feature is associated to the occurrence delamination phenomenon.

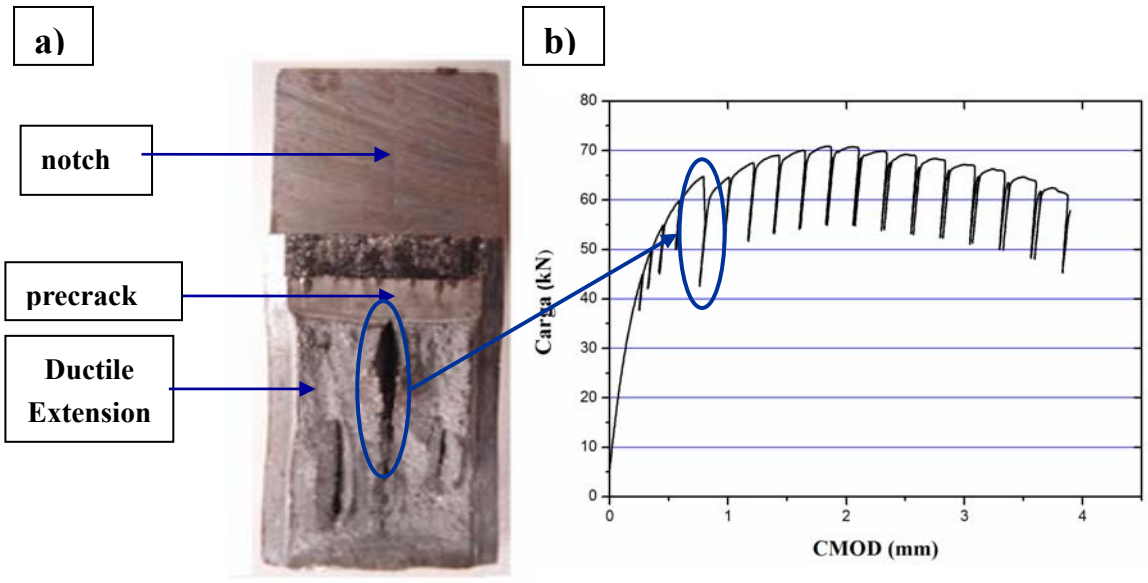

Figure 3. a) Fractured surface of sample from the fracture toughness test showing the notch, pre-fatigue and ductile extension, b) PxCMOD curve from the unloading compliance method indicating the occurrence of delamination on the curve.

Fig. 4.a shows the delamination region that was investigated by EBSD technique to obtaining of the microtexture. Fig. 4.b displays the orientation map, as well orientation triangle, where it can be observed a random grain sizes distribution from the rolling process occurred in the ($\alpha + \gamma$) range, as also the higher predominance of <111> and <100> orientations. Also in Fig. 4.b displays the remaining points may be perlite regions, which have very fine lamella (about 200nm). As the distance between lamellas is smaller than the step size used, the occurrence to indexation of crystallographic planes to these regions was not possible, resulting in dark regions. Another plausible explanation is associated to the material deformation, which can contribute to the accumulation of dislocations at grain boundaries, resulting in non-indexed regions.

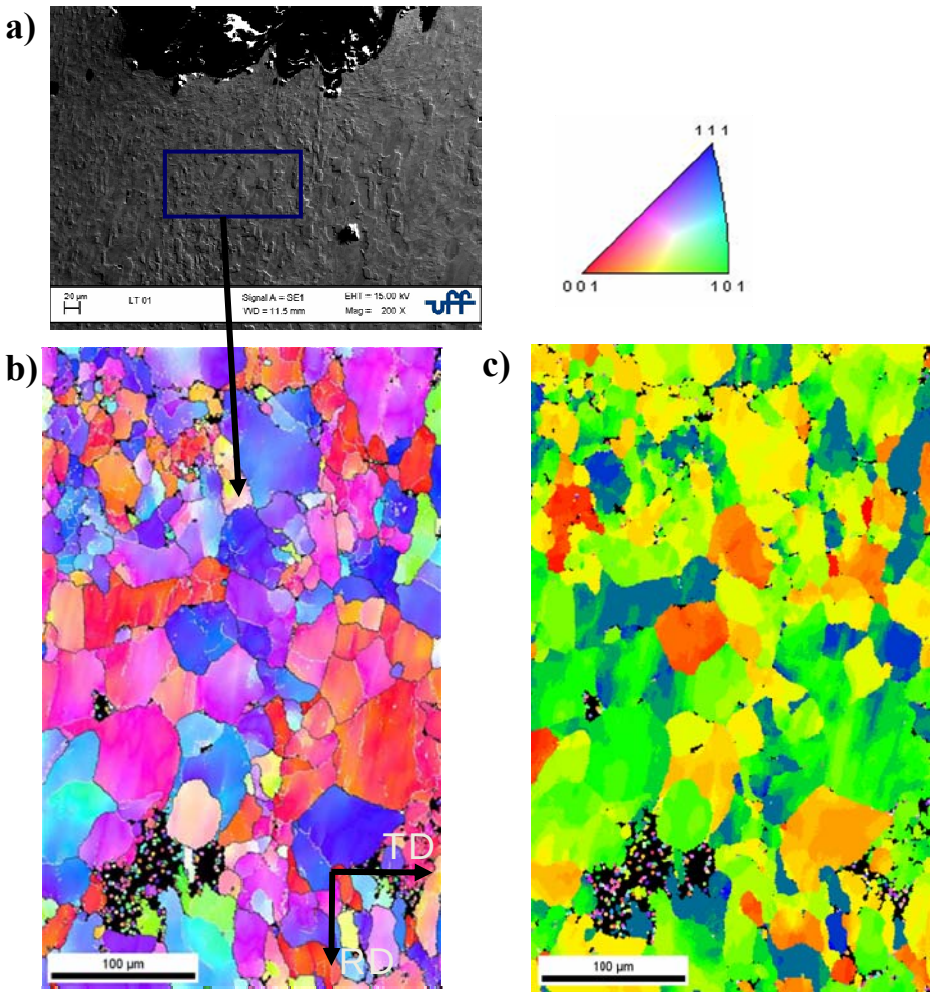

Figure 4. a) Delamination region used for microtexture analysis by EBSD technique b) orientation map of the selected region in the figure 3.a c) The Taylor factor Map of the same region.

Fig. 5 shows the Taylor factor distribution from the delamination region. It is possible to note the higher predominance of Taylor factor value between 2.5 to 3.5 corresponding 68% of grains. Moreover, 41% of grains have Taylor factor value lower 3 indicating lower absorbed energy. This indicates that the delamination phenomenon occur in the lower Taylor factor values. While the higher Taylor factor value (4) corresponded only 6% of grains.

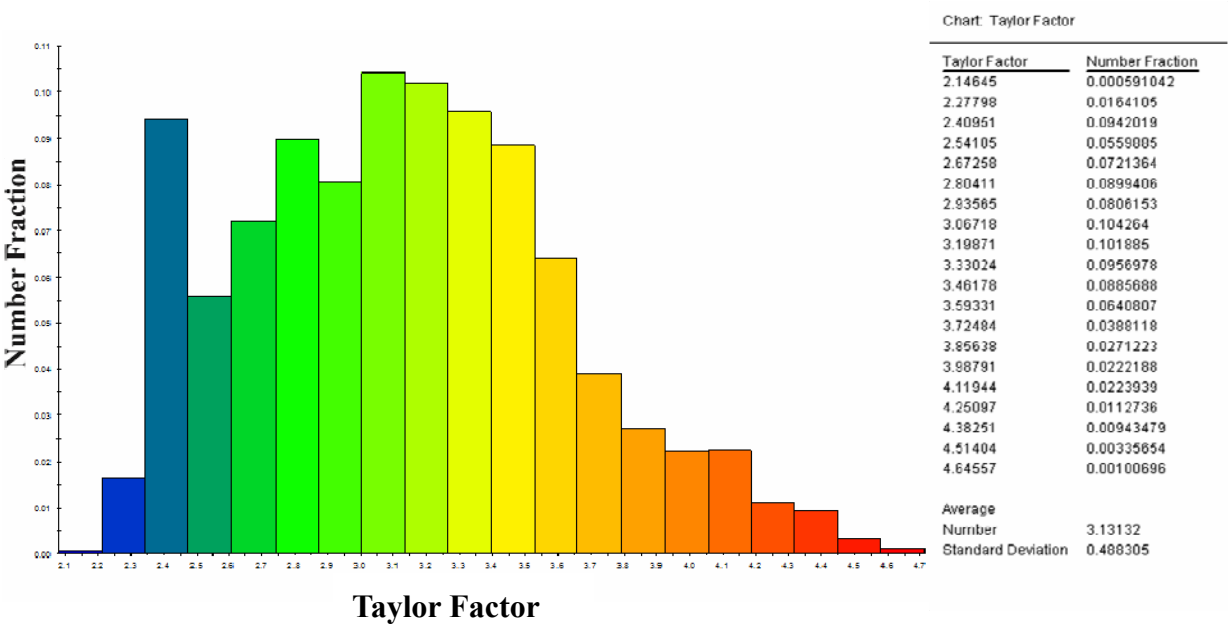

Figure 5. Histogram the Taylor factor distribution from Fig. 4.c.

Fig. 6.a shows the pole figures from the (111), (110) and (100) centered plans in the delamination region. Fig. 6.b shows the orientation distribution function (ODF) obtained for the section $\varphi_2 = 45$ °, which is the most important section on steels analysis, φ_1 is Euler angle aligned with RD while Φ is aligned to TD. The main components were obtained from ODF's because pole figures provide incomplete information [21]. It can be seen in Figs. 6.a and 6.b the formation of fiber texture: α fiber or fiber DL, γ fiber or fiber DN and cube textures. The presence these components are common in low carbon steel from the controlled rolling process. It can suffer change in the intensity value according to different processing and composition chemical of the steel [3].

The α fiber components more intense were: {113} <110>, {112} <110> and {223} <110>, which it can cause anisotropy mechanical properties [3, 5, 6]. This manner, the {113} <110> fiber component is generated from the deformed austenite recrystallization {112} <111> component. While the {112} <110> and {223} <110> fiber components both are produced by deformation from the {113}<110> rotation component. The same components can be contributing to ductile crack propagation during the test.

The cube fiber components were: {100} <120> and {100} <230>. These components usually are the lower intensity than γ and α fiber texture, this feature is attributed to recrystallization process [3]. The {100} <110> texture component was also found, the same is parallel to the rolling direction and contribute to both occurrence the cleavage plane and delamination phenomenon [3, 7, 8, 9, 10].

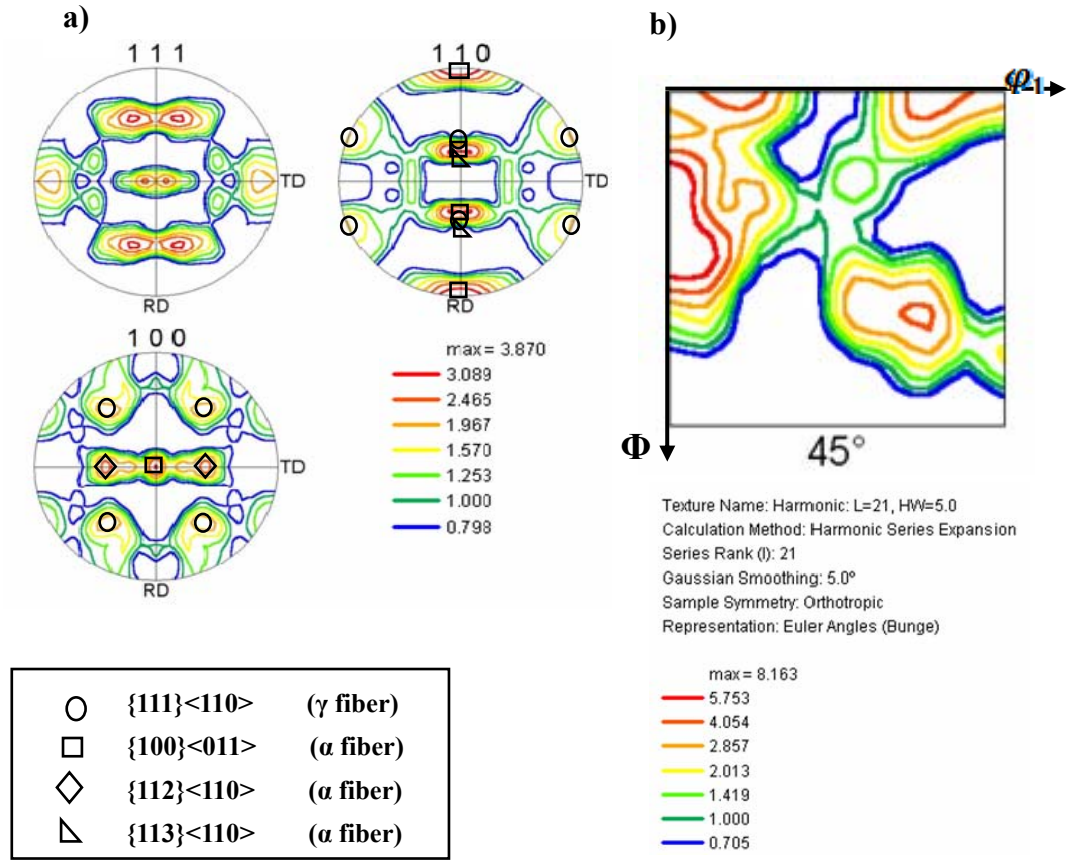

Figure 6. a) Pole figures from the (111), (110) and (100) centered planes obtained in the delamination region. b) orientation function o distribution for the section $\varphi_2 = 45°$.

5. Conclusions

The orientation maps close to the delamination region have displayed a heterogeneous grain size distribution. The Taylor factor values were the lower absorbed energy with <100> type orientation. While the <111> type orientation has shown higher absorbed energy, consequently, a higher Taylor factor value. The orientation distribution function and pole figure have shown the presence of the α fiber texture such as :{113}<110>, {112}<110> e {223}<110>, these components produce anisotropic mechanical properties that during fracture process act to reduce the plastic constraint and contributing to increase the stress plane. The {100}<110> cube fiber component has been found in the delamination region, it is main responsible to the occurrence of phenomenon in HSLA.

Acknowledgements

The authors thank the USIMINAS by providing the material under study, the UFF-Federal Fluminense University, for performing the EBSD measurements, and CAPES for providing scholarship and the project (Case No. PNPD-23038.008242/2010-08)

References

[1] Specification for line pipe steel API5L, API, 2007.
[2] D. Porter, A. Laukkanen, P. Nevasmaa, K. Rahka, K. Wallin, Performance of TMCP steel with respect to mechanical properties after cold forming and post-forming heat treatment. Int J Press Vessels Pip, 22 (2004) 867–877.
[3] R. K. Ray, J. J. Jonas, Transformation textures in steels. Int Mater Rev, 35 (1990) 1-36.
[4] F. J. Humphreys, M. Hatherly, Recrystallization and related annealing phenomena. Amsterdam, Elsevier, 2004.
[5] G.J. Baczynski, J.J. Jonas, L. E. Collins, The influence of rolling practice on notch toughness and texture development in high-strength linepipe. Metall Mater Trans A, 30 (1999) 3045 – 3054.
[6] P.K.C. Venkatsurya, Z. Jia, R.D.K. Misra, M.D.Mulholland, M. Manohar, J.E. Hartmann. Understanding mechanical property anisotropy in high strength niobium-microalloyed linepipe steels. Mater Sci Eng A, 556 (2012) 194-210.
[7] R.D.K. Misra, H. Nathani, F. Siciliano, Effect of texture and microstructure on resistance to cracking of high-strength hot-rolled nb-ti microalloyed steels. Metall Mater Trans A, 35 (2004) 3024-3029.
[8] D.L. Bourell, Cleavage delamination in impact tested warm-rolled**.** Metall Trans A, 14 (1983) 1983-2487.
[9] M.S. Joo, W. Suh, J.H. Bae, H.K.D.H. Bhadeshia, Role of delamination and crystallography on anisotropy of Charpy toughness in API-X80 steel. Mater Sci Eng A, 546 (2012) 314-322.
[10] T. Inoue, F. Yin, Y. Kimura, K. Tsuzaki, S. Ochiai, Delamination Effect on impact properties of ultrafine-grained low-carbon steel processed by warm caliber rolling. Metall Mater Trans A, 41 (2010) 341-355.
[11] W. Yan, W. Sha, L. Zhu, W. Wang, Y. Y. Shan, K. Yang, Delamination fracture related to tempering in a high-strength low-alloy steel. Metall Mater Trans A, 41 (2010) 159-171.
[12] T. Otárola, S. Hollner, B. Bonnefois, M. Anglada, L. Coudreuse, A. Embrittlement of a superduplex stainless steel in the range of 550–700 °C, Eng Fail Anal, 12 (2005) 930–941.
[13] T. Tanaka, Controlled rolling of steel plate and strip. Int Mater Rev, 4 (1981) 185-212.
[14] C. Grobler, G. T. Van Rooyen, The mechanisms by which splitting occurs along sheared edges and in charpy specimens of a 12% chromium steel, Can Metall Q, 27 (1988) 49- 58.
[15] B.L. Bramfitt, A.R. Marder, A study of the delamination behavior of a very low-carbon steel. Metall Mater Trans A, 8 (1977) 1263-1273.
[16] American Society for Test and Materials, Standard test method for tension test of metallic materials [metric], ASTM E8M, Philadelphia, 2004.
[17] American Society for Test and Materials. Standard test method for measurement of fracture toughness, ASTM E1820, Philadelphia, 2005.
[18] S. Cravero, C. Ruggieri, Estimation procedure of J-resistance curves for SE(T) specimens using unloading compliance. Eng Fract. Mech, 74 (2007) 2735-2757.
[19] E. Hippert Jr, Investigação experimental do comportamento dúctil de aços API-X70 e aplicação de curvas de resistência J-Δa para previsão de colapso em dutos. M. Sc. thesis, Polytechnic School of São Paulo, Univesity of São Paulo, 2007.
[20] W. Guo, H. Dong, M. Lu, X. Zhao, The coupled effects of thickness and delamination on

cracking resistance for X70 pipeline steel. Int J Press Vessels Pip, 79 (2002) 403 - 412.
[21] V. Randle, O. Engler, Introduction to Texture Analysis: macrotexture, microtexture, and orientation mapping, CRC Press, 2000.